Magnetism in Geometrically Frustrated $YMnO_3$ under Hydrostatic Pressure Studied with Muon Spin Relaxation

T. Lancaster,[1,*] S. J. Blundell,[1] D. Andreica,[2,†] M. Janoschek,[3,4] B. Roessli,[4] S. N. Gvasaliya,[4] K. Conder,[5] E. Pomjakushina,[4,5] M. L. Brooks,[1] P. J. Baker,[1] D. Prabhakaran,[1] W. Hayes,[1] and F. L. Pratt[6]

[1]*Clarendon Laboratory, Department of Physics, Oxford University, Parks Road, Oxford, OX1 3PU, United Kingdom*
[2]*Laboratory for Muon Spin Spectroscopy, Paul Scherrer Institut, CH-5232 Villigen, Switzerland*
[3]*Technische Universität München, Physics Department E21, D-85747 Garching, Germany*
[4]*Laboratory for Neutron Scattering, ETHZ and Paul Scherrer Institut, CH-5232 Villigen, Switzerland*
[5]*Laboratory for Developments and Methods, Paul Scherrer Institut, CH-5232 Villigen, Switzerland*
[6]*ISIS Facility, Rutherford Appleton Laboratory, Chilton, Oxfordshire OX11 0QX, United Kingdom*

(Received 17 October 2006; published 9 May 2007)

The ferroelectromagnet $YMnO_3$ consists of weakly coupled triangular layers of $S = 2$ spins. Below $T_N \approx 70$ K muon-spin relaxation data show two oscillatory relaxing signals due to magnetic order, with no purely relaxing signals resolvable (which would require different coexisting spin distributions). The transition temperature T_N increases with applied hydrostatic pressure, even though the ordered moment decreases. These results suggest that pressure increases both the exchange coupling between the layers and the frustration within the layers.

DOI: 10.1103/PhysRevLett.98.197203 PACS numbers: 75.25.+z, 75.40.Cx, 75.50.Ee, 76.75.+i

The hexagonal $RMnO_3$ manganites [1] (R = Ho, Er, Tm, Yb, Lu, Y, or Sc) are a class of magnetically ordered materials that also possess ferroelectric properties and some degree of magnetoelectric coupling, suggesting that an understanding of the magnetism may allow manipulation of the electric polarization with possible device applications [2]. Moreover, these compounds are layered and exhibit geometric frustration within their layers, offering the possibility of studying the effect of competing interactions in low-dimensional systems [3].

$YMnO_3$, an insulator which undergoes a ferroelectric transition at $T_E = 913$ K [4], is the most intensively studied of the $RMnO_3$ series. The magnetic system is based on a frustrated architecture, with Mn^{3+} ($S = 2$) ions forming a two-dimensional (2D) corner-sharing triangular network. Studies of magnetic susceptibility [5] confirm the frustrated nature of the system, with a large ratio of Weiss temperature ($|\Theta| = 705$ K) to antiferromagnetic (AFM) ordering temperature ($T_N \approx 70$ K). Neutron diffraction studies [6,7] have found that below T_N the Mn^{3+} spins lie in the ab plane and adopt a 120° structure, with a Mn moment of 2.9–3.1 μ_B at 1.7 K. This is below the expected value of 4 μ_B, due to fluctuations associated with either the frustration or the low dimensionality. Heat capacity measurements [5,8] suggested incomplete ordering of the Mn spins below T_N and elastic and inelastic neutron scattering (INS) measurements [9] found strong diffuse scattering persisting across T_N; this was taken as evidence for a spin-liquid phase which coexists with the ordered phase below T_N. However, it has been claimed that by taking low energy Einstein modes into account, heat capacity data may be consistent with conventional AFM ordering [10]. Other INS studies [11,12] have found evidence for coexisting three-dimensional (3D) and 2D fluctuations. More recent neutron studies [13,14] show that the ordered moment decreases with increasing hydrostatic pressure. This observation was explained in terms of a pressure-induced change in volume fraction of ordered and spin-liquid components of the material [13].

In this Letter we present the results of muon-spin relaxation [15] (μ^+SR) measurements made on $YMnO_3$ at ambient pressure and as a function of hydrostatic pressure p up to $p = 13.7$ kbar. Muons are a sensitive local probe of the spin distributions in a magnetic material and have proven particularly useful in probing frustration related effects [16]; however, measurements made under pressure have been less common. Strikingly, we show that T_N increases with increasing p, even though the magnetic moment decreases. This provides, as we shall show, an insight into the role of the finely balanced interactions in this system.

Zero-field (ZF) μ^+SR measurements [17] were made on a single crystal sample of $YMnO_3$ using the GPS instrument at the Swiss Muon Source (SμS) and on the MuSR instrument at the ISIS facility. The muon spin was directed along the crystallographic c axis of the sample. Transverse field (TF) μ^+SR measurements were made on a powder sample of $YMnO_3$ under hydrostatic pressure using high energy incident muons on the μE1 decay muon beam line at SμS. For these measurements, the sample was packed into a cylinder approximately 7 mm in diameter and 18 mm in length which was mounted in a Cu-Be25 piston cylinder pressure cell with Daphne oil used as the pressure medium. The pressure was measured by monitoring the superconducting transition temperature of an indium wire located in the sample space [18].

Example ZF μ^+SR spectra at ambient pressure (measured at SμS) are shown in Fig. 1. Below T_N we observe oscillations in the time dependence of the muon polarization (the "asymmetry" [15]) characteristic of a quasistatic

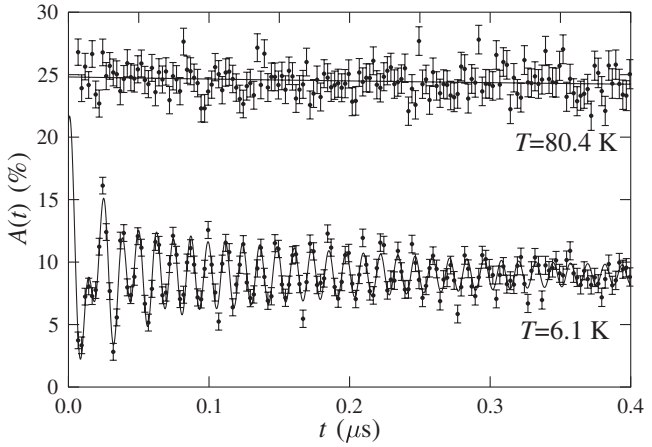

FIG. 1. ZF μ^+SR spectra measured at $T = 6.1$ and 80.4 K at $p = 1$ bar, with oscillations clearly observable below T_N.

local magnetic field at the muon stopping site. This local field causes a coherent precession of the spins of those muons with a component of their spin polarization perpendicular to this local field. The frequency of the oscillations is given by $\nu_i = \gamma_\mu B_i/2\pi$, where γ_μ is the muon gyromagnetic ratio ($=2\pi \times 135.5$ MHz T^{-1}) and B_i is the average magnitude of the local magnetic field at the ith muon site. Any fluctuation in magnitude of these fields will result in a relaxation of the signal, described by relaxation rates λ_i. Two separate frequencies were identified in the low temperature spectra, corresponding to two magnetically inequivalent muon stopping sites in the material. The larger frequency ν_1 is found to have a small relaxation rate λ_1 while the smaller frequency ν_2 is associated with a relaxation rate λ_2 which is an order of magnitude larger. The spectra were found to be well fitted using only oscillatory components. In the ordered phase of $YMnO_3$ the Mn^{3+} moments adopt the 120° structure, where the ordered Mn moments lie within the a-b plane [6]. Although the initial muon polarization is directed parallel to the c direction, the fact that the muon couples to dipole fields means that, in addition to the magnetic field components directed perpendicular to the muon spin, there may also exist components parallel to the muon spin. In our measurements these components only give rise to a constant background offset.

To follow the temperature evolution of the observed features the SμS spectra below T_N were fitted to the functional form

$$A(t) = A_{\mathrm{bg}} + \sum_{i=1}^{2} A_i e^{-\lambda_i t} \cos(2\pi\nu_i t + \phi_i), \qquad (1)$$

where A_{bg} represents a constant background contribution, including the signal from those muons that stop in the silver sample holder or cryostat tails. Nonzero phases ϕ_i were required to fit the observed oscillations because of the difficulty in resolving features at early times in the spectra due, at least in part, to the fast initial depolarization feature. To give the best fit across the entire temperature range we fixed $A_1 = 4.0\%$, $\phi_1 = -34°$ $A_2 = 8.8\%$, and $\phi_2 = -19°$.

We are unable to resolve a relaxing signal due to any coexisting spin distribution such as the spin-liquid phase suggested to persist into the ordered phase [9]. Our muon data are straightforwardly accounted for by a model assuming conventional long range magnetic order throughout the bulk of the sample. The full muon asymmetry is observed above T_N and relaxes exponentially with a single relaxation rate, as expected for a conventional paramagnetic state. Below T_N we observe an oscillatory signal with only weak relaxation, as expected for a well-defined magnetically ordered state. Thus we find no evidence for any static magnetic inhomogeneities in our sample, nor any evidence for coexisting ordered and disordered volume fractions. Furthermore, simulations of the internal field distribution expected from ''droplets'' of spin liquid dispersed in an antiferromagnetic medium predict a sizeable slowly relaxing fraction, inconsistent with our data. This effectively rules out a model in which long range order and a disordered spin liquid somehow coexist in different regions of the sample. Thus the diffuse scattering observed in neutron experiments [9] (which has been proposed to arise from a spin-liquid state) results not from phase separated regions but more likely from high frequency fluctuations which are motionally narrowed on the muon time scale and which do not affect the magnetic ground state of the system. Our data do show a small missing fraction of relaxing asymmetry (approximately 10% of the total signal) corresponding to muons which are depolarized within 1 ns of implantation (not resolvable in our measurements), but this feature only appears below T_N, unlike the diffuse scattering which persists across the transition [9].

Complementary data were measured over a longer time window at the ISIS facility, where the limited time resolution does not allow us to resolve oscillations. Instead, we see a sharp decrease in the relaxing amplitude A_{rel} as the material is cooled through T_N. This is because the local field in the ordered state will strongly depolarize the muon spin if local field components are perpendicular to the initial muon-spin polarization (or have no effect on it if local field components are parallel to the initial muon-spin polarization), removing the relaxing asymmetry from the spectrum. These data [Fig. 2(a)] show that the relaxing amplitude does not vary with temperature apart from at T_N, showing that there is no temperature variation in the volume fractions due to the ordered magnetic state (for $T < T_N$) or paramagnetic state ($T > T_N$). Moreover, only a weak, temperature independent relaxation (≈ 0.015 MHz) is observed in the ISIS data below T_N, which is well within the ordinarily expected background contribution, confirming that no purely relaxing component is needed in Eq. (1).

Figure 2(b) shows that ν_1 and ν_2 can be fitted by $\nu_i(T) = \nu_i(0)(1 - (T/T_N)^\alpha)^\beta$ from which we estimate $T_N = 74.7(3)$ K, $\alpha \approx 2.5$, and $\beta = 0.35(3)$, consistent

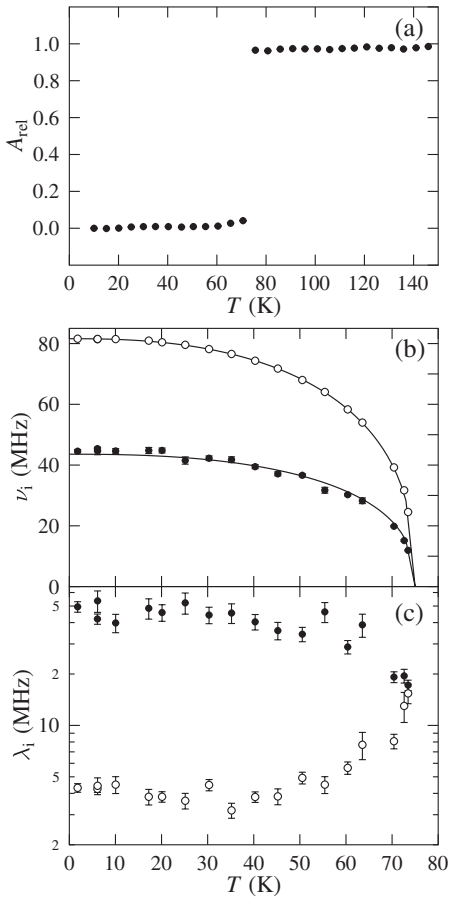

FIG. 2. (a) Relaxing asymmetry (normalized) A_{rel} (measured at ISIS) showing a steplike change at T_N (see text). (b),(c) Fits of the SμS spectra at $p = 1$ bar to Eq. (1). (b) Temperature dependence of precession frequencies ν_1 (open circles) and ν_2 (solid circles). The solid line is a fit to $\nu_i(T) = \nu_i(0)(1 - (T/T_N)^{\alpha})^{\beta}$ (see main text). (c) Relaxation rates λ_1 (open circles) and λ_2 (solid circles).

with 3D Heisenberg or 3D XY behavior, as found in specific heat studies [10]. Our determination of $\nu_i(0)$ allows us to attempt to identify the muon sites in $YMnO_3$. Dipole fields were calculated in a sphere containing $\sim 10^5$ Mn ions with moments of $2.9\mu_B$ arranged in the 120° structure. The positive muon's position is usually in the vicinity of electronegative O^{2-} ions [19]. Candidate muon sites giving rise to the higher oscillation frequency ν_1 are found to be separated from an O(4) oxygen by 1 Å along the c direction. This gives sites at coordinates $(1/3, 2/3, z)$ and $(2/3, 1/3, z)$, where $z \approx 0.09$, 0.42, 0.59, and 0.92. Several candidate sites for the lower frequency ν_2 are found close to the planes of triangularly arranged O(1) and O(2) atoms. One possibility is for the sites to lie between oxygens, with the sites forming triangles centered again on the $(1/3, 2/3, z)$ and $(1/3, 2/3, z)$ positions, where now $z \approx 0.18$ and ≈ 0.32.

The division of the muon sites into a set lying close to the Mn planes and a set between these planes may explain the difference in the observed relaxation rates. The relaxation rates are expected to vary as $\lambda \sim \Delta^2\tau$, where Δ is the second moment of the local magnetic field distribution and τ is its fluctuation time. Sites giving rise to the frequency ν_1 lie close to the Mn planes in well-defined positions such that Δ is small. We also expect muons at these sites to be sensitive to both in-plane (2D) and out-of-plane (3D) magnetic fluctuations. Relaxation rate λ_1 increases as T_N is approached from below [Fig. 2(c)] because τ increases due to the onset of critical fluctuations close to the phase transition. Sites associated with frequency ν_2 lie between the Mn planes in several positions where there is some variation of the dipole fields around 40 MHz and consequently a large value of Δ. These will be less sensitive to 2D fluctuations than those lying close to the planes, reducing the influence of any variation in τ. The temperature evolution of λ_2 [Fig. 2(c)] is now dominated by the magnitude of Δ, which scales with the size of the local field. Relaxation rate λ_2 therefore decreases as the magnetic transition is approached from below.

In contrast to the ZF data measured at ambient pressure at SμS, it is not possible to resolve precession frequencies in SμS ZF data measured under hydrostatic pressure. This is because the signal from the sample amounts to only 20% of the total measured spectrum from the pressure cell and is strongly depolarized. To observe the magnetic transition, it was necessary to follow the amplitude of the muon precession in a transverse field of $B_t = 5$ mT [Fig. 3(a)] and fit the data to the functional form $A(t) = [A_0 + (A_\infty - A_0)A_{\mathrm{rel}}]e^{-\Lambda t}\cos(\gamma_\mu B_t t)$, where A_0 and A_∞ are found to be independent of pressure, Λ is a relaxation rate, and A_{rel} is the normalized amplitude. The temperature dependence of A_{rel} characterizes the magnetic transition and is shown in Fig. 3(b) for several applied pressures. The pressure independence of A_0 and A_∞ are inconsistent with an earlier speculation [13] that there is a change in volume fraction between spatially separated spin-liquid and AFM states when the pressure is varied. To extract the transition temperature we use the phenomenological form $A_{\mathrm{rel}} = [1 + \exp(-b\{T - T_N\})]^{-1}$, where b is a parameter describing the "width" of the transition. At all pressures the parameter b remained practically unchanged at $b \approx 1.2\ \mathrm{K}^{-1}$, while T_N shows a linear increase with pressure as shown in Fig. 3(c). A straight line fit yields $T_N = 74.0 + 0.29p$, where p is the pressure in kbar. Our value for $dT_N/dp = 0.29\ \mathrm{K\,kbar}^{-1}$ is in excess of that predicted by the "10/3" law [20], $dT_N/dp = (10/3)T_N/\mathcal{B}$ (where $\mathcal{B}$ is the bulk modulus), which holds for many oxides and garnets. Using $\mathcal{B} = 1.65$ Mbar [21] yields an estimate $dT_N/dp = 0.14\ \mathrm{K\,kbar}^{-1}$, which is approximately half the measured value. This strong pressure dependence of T_N demonstrates the sensitivity of T_N to pressure-induced small changes in intralayer J and interlayer coupling J' (see, e.g., Ref. [22]).

The increase of T_N with pressure in $YMnO_3$ is surprising given that previous studies [13,14] have shown that the

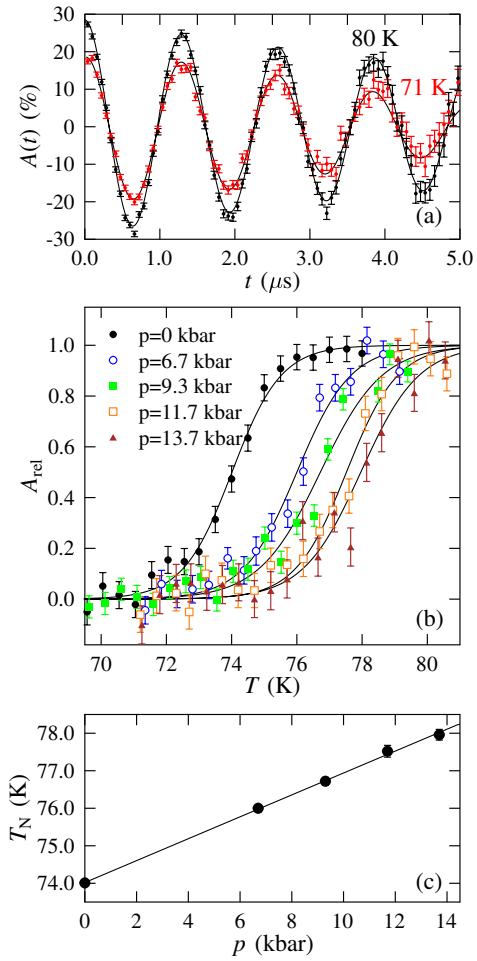

FIG. 3 (color online). Results of TF μ^+SR measurements made under hydrostatic pressure. (a) Example spectra measured at $p = 11.7$ kbar in a TF of 5 mT at $T = 71$ K [gray (red) circles] and $T = 80$ K (black circles). (b) Temperature dependence of the normalized amplitude, A_{rel}, for several applied pressures. (c) The transition temperature T_N is seen to increase linearly with increasing pressure.

magnitude of the ordered moment decreases with applied pressure, implying an increase in the spin fluctuations that reduce the value of the magnetic moment found at ambient pressure. It is plausible that the application of hydrostatic pressure to the polycrystalline material has two effects. The first is on the structure of the triangular MnO planes as shown by neutron measurements [13]. At ambient pressures the Mn-O(3)-Mn and Mn-O(4)-Mn bond angles and length differ slightly. This relieves the magnetic frustration to an extent. The neutron diffraction measurements show that upon the application of pressure the Mn-O(3)-Mn and Mn-O(4)-Mn bond angles and lengths approach each other. These effects act to make the MnO planes more perfect realizations of a triangular lattice, causing the exchange coupling along the triangular bonds to become more similar as pressure is increased. This increased frustration has been proposed as an explanation for the reduction in magnetic moment [13,14]. The second effect is an increase in both J' and J, which have an exponentially sensitive dependence on bond distance, making the relative effect on J' larger. INS measurements at ambient pressure show that $J'/J \sim 10^{-2}$ [11], which is consistent with $T_N/J \sim 0.5$ ($J \approx 3$ meV [9,11]). Pressure will therefore increase J'/J and hence T_N. It is clear that in order for this dual effect to occur there exists a delicate balance of competing interactions in this system.

This work was carried out at SμS, Paul Scherrer Institut, Villigen CH and at the ISIS facility, Rutherford Appleton Laboratory, U.K. We thank Hubertus Luetkens for technical assistance and EPSRC (U.K.) for financial support. T. L. thanks the Royal Commission for the Exhibition of 1851 for support.

*Electronic address: t.lancaster1@physics.ox.ac.uk
†On leave from: Faculty of Physics, Babes-Bolyai University, 400084 Cluj-Napoca, Romania.

[1] H. Yakel *et al.*, Acta Crystallogr. **16**, 957 (1963).
[2] W. Eerenstein *et al.*, Nature (London) **442**, 759 (2006).
[3] R. Moessner, Can. J. Phys. **79**, 1283 (2001).
[4] D. Fröhlich *et al.*, Phys. Rev. Lett. **81**, 3239 (1998).
[5] T. Katsufuji *et al.*, Phys. Rev. B **64**, 104419 (2001).
[6] A. Muñoz *et al.*, Phys. Rev. B **62**, 9498 (2000).
[7] P. J. Brown and T. Chatterji, J. Phys. Condens. Matter **18**, 10 085 (2006).
[8] D. G. Tomuta *et al.*, J. Phys. Condens. Matter **13**, 4543 (2001).
[9] J. Park *et al.*, Phys. Rev. B **68**, 104426 (2003).
[10] M. Tachibana *et al.*, Phys. Rev. B **72**, 064434 (2005).
[11] T. J. Sato *et al.*, Phys. Rev. B **68**, 014432 (2003).
[12] B. Roessli *et al.*, JETP Lett. **81**, 287 (2005).
[13] D. P. Kozlenko *et al.*, JETP Lett. **82**, 193 (2005).
[14] M. Janoschek *et al.*, J. Phys. Condens. Matter **17**, L425 (2005).
[15] S. J. Blundell, Contemp. Phys. **40**, 175 (1999).
[16] F. Bert *et al.*, Phys. Rev. Lett. **97**, 117203 (2006); P. Dalmas de Réotier *et al.*, Phys. Rev. Lett. **96**, 127202 (2006); X. G. Zheng *et al.*, Phys. Rev. Lett. **95**, 057201 (2005).
[17] Data were measured in 8192 bins, each of width 1.25 ns.
[18] Samples were produced via a solid state reaction. Stoichiometric mixtures of Y_2O_3 and MnO_2 were ground together and calcined in air. For the polycrystalline material this process lasted 70 hours at ~1200 °C with several intermediate grindings. The single crystal material was pressed into a rod under 60 MPa hydrostatic pressure and crystals were grown in an optical floating zone furnace (Crystal System, Inc.) at a growth speed of 5 mm/h, with the seed and feed rods counterrotating at 25 rpm. Purity was confirmed with x-ray diffraction.
[19] E. Holzschuh *et al.*, Phys. Rev. B **27**, 5294 (1983).
[20] D. Bloch, J. Phys. Chem. Solids **27**, 881 (1966).
[21] A. Posadas *et al.*, Appl. Phys. Lett. **87**, 171915 (2005).
[22] J. W. Lynn *et al.*, Phys. Rev. B **40**, 5172 (1989).